

Early and persistent activation of myocardial apoptosis, *bax* and caspases: insights into mechanisms of progression of heart failure

Gordon W. Moe^{a,*}, George Naik^a, Andrea Konig^a, Xiangru Lu^b, Qingping Feng^b

^a Department of Medicine, Division of Cardiology, St. Michael's Hospital, Terrence Donnelly Heart Center, University of Toronto, 30 Bond Street, Toronto, Ontario, Canada M5B1W8

^b Department of Medicine, The University of Western Ontario, London, Ontario, Canada

Received 15 October 2001; received in revised form 11 December 2001; accepted 25 December 2001

Abstract

The aim of this study was to test the hypothesis that persistent myocardial apoptosis contributes to progression of heart failure in a canine model of pacing-induced cardiomyopathy. Dogs were paced at 250 beats per minute for 1 week ($n = 9$), 3 weeks ($n = 14$) and 4 weeks ($n = 14$) with normal dogs served as controls ($n = 12$). Myocardial apoptosis was assessed by multiple methods including DNA fragmentation and in situ terminal deoxynucleotidyl transferase-mediated dUTP nick end labeling (TUNEL) staining, *bax* and *bcl-2* protein expression, and caspase activity. Pacing produced a progressive increase in left ventricular (LV) end diastolic pressure (LVEDP) and plasma norepinephrine levels with no significant increase in LV mass. The number of apoptotic cells was markedly increased after 1 week of pacing and remained increased at 4 weeks of pacing with characteristic DNA laddering. The increase in apoptosis was associated with *bax* protein expression and caspase activation while there was no detectable changes in *bcl-2* protein expression. The estimated total number of apoptotic cells correlated with cardiac output and LVEDP ($r = -0.69$ and 0.59 , respectively, $P < 0.001$). Plasma norepinephrine and *bax* protein expression correlated significantly with the estimated total number of apoptotic myocytes ($r = 0.62$ and 0.42 , respectively, $P < 0.01$). In conclusion, an early and persistent activation of myocardial apoptosis and pro-apoptotic factors is likely an important mechanism that contributes to the progression of heart failure in canine pacing-induced cardiomyopathy. © 2002 Elsevier Science Ireland Ltd. All rights reserved.

Keywords: Heart failure; Progression; Apoptosis; Cytokines; Myocytes

1. Introduction

Chronic heart failure is a disorder that is characterized by a relentless progressive course [1]. Accordingly, further understanding of the mechanisms mediating the progression of heart failure is important. It is currently believed that the activation of neurohormonal mechanisms and the pro-inflammatory cytokines is important in mediating the progression of heart failure [2,3]. One potentially important and yet unproven mechanism for the progression of heart failure is an ongoing loss of myocardial cells. Apoptosis, or programmed cell death, may be one of the mechanisms responsible for continuing loss of myocytes in chronic heart failure. The

hallmark of apoptosis is a fragmentation of chromosomal DNA [4]. This process of DNA fragmentation is associated with the abnormal expression of genes such as *Fas* [5], wild-type p53 [6], *c-myc* protein and *bax* [7], whereas *bcl-2* is known to inhibit apoptosis by forming heterodimers with *bax* [8]. Myocardial apoptosis has been observed in a variety of pathologic conditions such as myocardial ischemia–reperfusion injury, acute myocardial infarction [9,10], and in explanted hearts of patients with end stage heart failure [11,12].

Rapid pacing in the dog induces a heart failure syndrome with clinical, radiographic, echocardiographic and hemodynamic changes that closely mimic human heart failure [13,14]. One of the hallmarks of this model is a rapidly progressive course without preceded by adaptive cardiac hypertrophy at the whole-organ level [13,14]. Furthermore, heart failure is accompanied by intense hemodynamic stress and activation of neuro-

* Corresponding author. Tel.: +1-416-8645319; fax: +1-416-8645941.

E-mail address: moegord@attglobal.net (G.W. Moe).

hormonal systems as well as the pro-inflammatory cytokines including tumor necrosis factor-alpha (TNF- α) [14], factors that have been shown to trigger apoptosis [15]. Accordingly, the principal aim of our study was to test the hypothesis that myocardial apoptosis contributes to heart failure progression. To achieve this aim, we specifically examined myocardial apoptosis, expression of *bax* and *bcl-2*, promoter and inhibitor of apoptosis, respectively, as well as the activity of caspases, the executioner of apoptosis in normal and dogs at three stages of heart failure. These three stages were (1) early and clinically silent heart failure, (2) moderately heart failure, and (3) advanced and clinically overt heart failure. To assess the functional implication of apoptotic cell death, total number of apoptotic cells at each stage of heart failure was estimated and correlated with hemodynamic changes as a measure of heart failure progression.

2. Methods

2.1. Study groups

The study groups consisted of four groups of dogs. Twelve normal dogs not subjected to pacing served as controls. A second group of nine dogs underwent continuous rapid right ventricular pacing for 1 week was designated as the group with early heart failure. A third group of 14 dogs and a fourth group of 14 dogs, paced for 3 and 4 weeks, respectively, were designated as dogs with moderately severe and advanced heart failure, respectively. Approval was obtained from the institutional animal research committee before study commencement, in accordance with the guidelines on the *Care and Use of Experimental Animals* issued by the Canadian Council on Animal Care, Ottawa, Canada.

2.2. In vivo studies

The method of induction of heart failure, clinical and hemodynamic and echocardiographic assessments have been described in detail in previous reports [13,14,16]. Two-dimensional echocardiography and arterial blood sampling was performed weekly to monitor changes in left ventricular (LV) ejection fraction and for measurements of plasma norepinephrine and TNF- α levels. Hemodynamics were obtained using a high-fidelity catheter introduced via the femoral artery. Ultrasonographically derived LV mass were calculated at end-diastole using the formula for a hemispheric cylinder [17,18]. After the terminal in vivo study, the dogs were euthanized and tissue of the lateral wall of the LV was obtained and stored in -80°C until assessment.

2.3. Assays for norepinephrine and TNF- α

Plasma norepinephrine level was measured by a high-performance liquid chromatographic method described previously [19]. Plasma TNF- α level was determined by an enzyme-linked immunosorbent assay technique using a commercially available mouse TNF- α DuoSet kit (Genzyme Diagnostics, Cambridge, MA). Monoclonal hamster anti-mouse and horseradish peroxidase conjugated goat anti-mouse TNF- α antibodies were used in the assay.

2.4. Analysis of myocardial apoptosis

As each method of assessing apoptosis may have its inherent limitations, more than one method of study apoptosis were employed.

2.4.1. Microscale analysis of genomic DNA fragmentation

Genomic DNA fragmentation was determined using dideoxynucleotide [$\alpha^{32}\text{P}$]-ddATP labeling described by Tilley and Hsueh [20]. The labeled DNA was electrophoretically separated on a 1.5% agarose gel. Gels were dried and exposed to Kodak X-omat films at -80°C .

2.4.2. In situ 3'-end-labeling of DNA

To localize and quantitatively assess cells undergoing nuclear DNA fragmentation, in-situ terminal deoxynucleotidyl transferase-mediated dUTP nick end labeling (TUNEL) assay was performed on paraffin tissue sections using an in situ cell death detection kit according to the manufacturer's specifications (Boehringer Ingelheim, Burlington, ON, Canada). Sections were counter-stained with hematoxylin. Each slide was examined by light microscopy at $1000\times$ in 50 fields. Apoptosis was expressed as the number of apoptotic nuclei per 1000 nuclei. To identify cardiomyocytes and apoptotic nuclei of cardiomyocyte origin, sections were stained overnight at 4°C with a monoclonal ventricular heavy chain anti-myosin antibody (Chemicon, Temecula, CA, USA) before TUNEL staining was performed. For visualization, a rhodamine-conjugated secondary anti-mouse antibody was used. Apoptotic nuclei were visualized microscopically as green under fluorescein light and myosin was seen as red under rhodamine light.

2.4.3. Assessment of *bax* and *bcl-2* protein expression

Immunohistochemical staining for *bax* and *bcl-2* proteins in paraffin embedded sections ($5\ \mu\text{m}$) was performed according to a standard protocol [21]. Primary antibodies were monoclonal mouse anti-*bcl-2* (Santa Cruz Biotechnology, CA, USA) and polyclonal anti-*bax* (Transduction Laboratory). Specific immunoreactivity was detected using $1\ \text{mg/ml}$ 3,3'-diaminobenzidine tetrahydrochloride. The slides were then

counterstained with hematoxylin. Semi-quantitative grading (from 0 to 5) were performed by two experienced observers using light microscopy. Average grading of the two observers was used for data analysis. Western blot analysis for *Bax* and *bcl-2* protein expression was performed according to a standard protocol using the same antibodies as above. *Bax* and *bcl-2* proteins were detected as 21 and 26 kDa bands, respectively, using enhanced chemiluminescence detection reagents.

2.4.4. Caspase activity

Myocardial caspase activity (DEVDase) was measured by using a caspase-3 assay kit according to manufacturer's protocol (BIOMOL Research Laboratories, PA, USA). The assay is based on spectrophotometric detection of the chromophore ρ -nitroaniline (ρ NA) after cleavage from the labeled substrate Ac-DEVD- ρ NA. Since Ac-DEVD- ρ NA is also a substrate for caspase-3, the caspase activity measure represents the activity of both caspase-3 and 7.

2.5. Statistical analysis

Data were expressed as mean \pm Standard Error of Mean (S.E.M.) Comparison between the four study groups were performed by one-way ANOVA followed by a Newman–Keuls multiple comparison test or Dunn's method using GB-STATTM (Dynamic Microsystems, Inc, Silver Spring, MD, USA). A probability value of <0.05 was considered statistically significant.

3. Results

3.1. In vivo measurements

Development of heart failure in the paced dogs was confirmed by clinical, radiographic and hemodynamic assessments. Hemodynamic, echocardiographic and neurohormonal data for the control normal dogs, and dogs paced for 1 week (early heart failure), 3 and 4

weeks (severe heart failure) are shown in Table 1. In the control and 1 week-paced dogs, clinical signs of heart failure were not observed. In the dogs paced for 1 week, there was a modest increase in LV end diastolic pressure, accompanied by a decline in cardiac output ($P < 0.05$). In the 3 weeks paced-dogs, ten of the 14 dogs had two of the three clinical signs of apathy, anorexia and ascites. In the 4 weeks paced-dogs, all dogs developed at least two of the three signs of apathy, anorexia and ascites. After 3 and 4 weeks, LV end diastolic pressure increased and cardiac output decreased markedly, indicating a progressive increase in hemodynamic stress. These changes of severe heart failure were also accompanied by radiographic evidence of pulmonary edema and cardiomegaly. With the development of heart failure, there was a progressive increase in plasma norepinephrine levels signifying neurohormonal activation. Data for plasma TNF- α levels for each group are shown in Table 1. As heart failure evolved, there was a progressive increase in plasma TNF- α levels indicating increasing activation of this cytokine system. However, in spite of the intense hemodynamic stress and neurohormonal activation, there was no significant change in two-dimensional ultrasonically derived LV mass, indicating no significant LV hypertrophy had developed at least at the whole organ level.

3.2. DNA laddering

An example of genomic DNA fragmentation obtained by microscale autoradiography is depicted in Fig. 1. Equal loading of DNA in each lane was confirmed by ethidium bromide staining at the end of electrophoresis (data not shown). Characteristic DNA fragmentation in multiple of approximately 200 bp were observed in dogs paced for 1, 3 and 4 weeks but none in the control group.

3.3. Myocyte apoptosis

The number of cardiomyocyte nuclei with DNA fragmentation was detected by TUNEL staining. An

Table 1
In vivo hemodynamic, morphological and neurohormonal parameters

| | Controls | 1 week-pacing | 3 week-pacing | 4 week-pacing |
|-------------------------------|---------------|----------------------------|----------------------------|------------------------------|
| LVEDP (mmHg) | 10 \pm 1 | 24 \pm 1 ^a | 29 \pm 2 ^b | 40 \pm 2 ^{b,c} |
| Cardiac output (l/min) | 3.5 \pm 0.1 | 2.6 \pm 0.1 ^a | 2.5 \pm 0.1 ^b | 1.7 \pm 0.1 ^{b,c} |
| Plasma Norepinephrine (pg/ml) | 190 \pm 25 | 528 \pm 84 ^a | 650 \pm 78 ^b | 722 \pm 68 ^b |
| Plasma TNF α (pg/ml) | 8 \pm 4 | 79 \pm 27 ^a | 89 \pm 25 ^b | 247 \pm 98 ^{b,c} |
| LV mass (g/kg) | 2.6 \pm 0.2 | 2.7 \pm 0.2 | 2.6 \pm 0.2 | 2.8 \pm 0.1 |

Data are means \pm S.E.M. LVEDP, left ventricular end diastolic pressure.

^a $P < 0.05$.

^b $P < 0.001$ vs. controls.

^c $P < 0.05$ vs. 1 week-pacing.

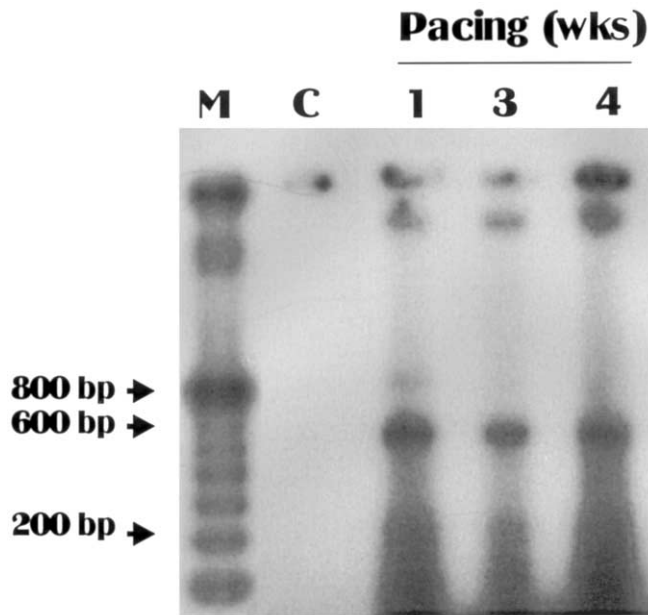


Fig. 1. Fragmentation of genomic DNA on an agarose gel. Genomic DNA was isolated from LV myocardium in control (C) and the paced dogs. One μg DNA was loaded in each lane. M, DNA molecular marker.

example of TUNEL and myosin heavy chain double staining is depicted in Fig. 2. A typical apoptotic nucleus is shown in green (Fig. 2A). The apoptotic nuclei were quantified in relation to normal nuclei in 50 high power ($1000\times$) fields. As shown in Fig. 3A, in the control dogs, there were very few apoptotic nuclei. After only 1 week of pacing (early heart failure), there was a significant increase in the number of apoptotic nuclei ($P < 0.05$). This increase persisted in the 3 and 4 week-paced dogs with more severe heart failure ($P < 0.05$).

3.4. Estimation of total apoptotic cells

Using the TUNEL stain data, a hypothetical estimation of total myocyte cell loss due to apoptosis was calculated based on the following assumptions. First, the total number of ventricular cardiomyocytes in a dog heart was 2.4×10^9 , as reported by Liu et al. [22]. Second, two apoptotic nuclei equaled one apoptotic cardiomyocyte in the paced dogs, based on the report by Kajstura et al. [23]. Third, apoptosis was completed in 12 h [24]. Fourth, the rate of apoptosis measured at 1, 3 and 4 weeks after pacing represented the average rate of apoptosis for 1, 3 and 4 weeks, respectively. The total number of apoptotic cells (Y) was then calculated according the following equation:

$$Y = \sum_{i=1}^n \frac{M(1 - X)^{i-1} X}{2}$$

M was the total number of ventricular cardiomyo-

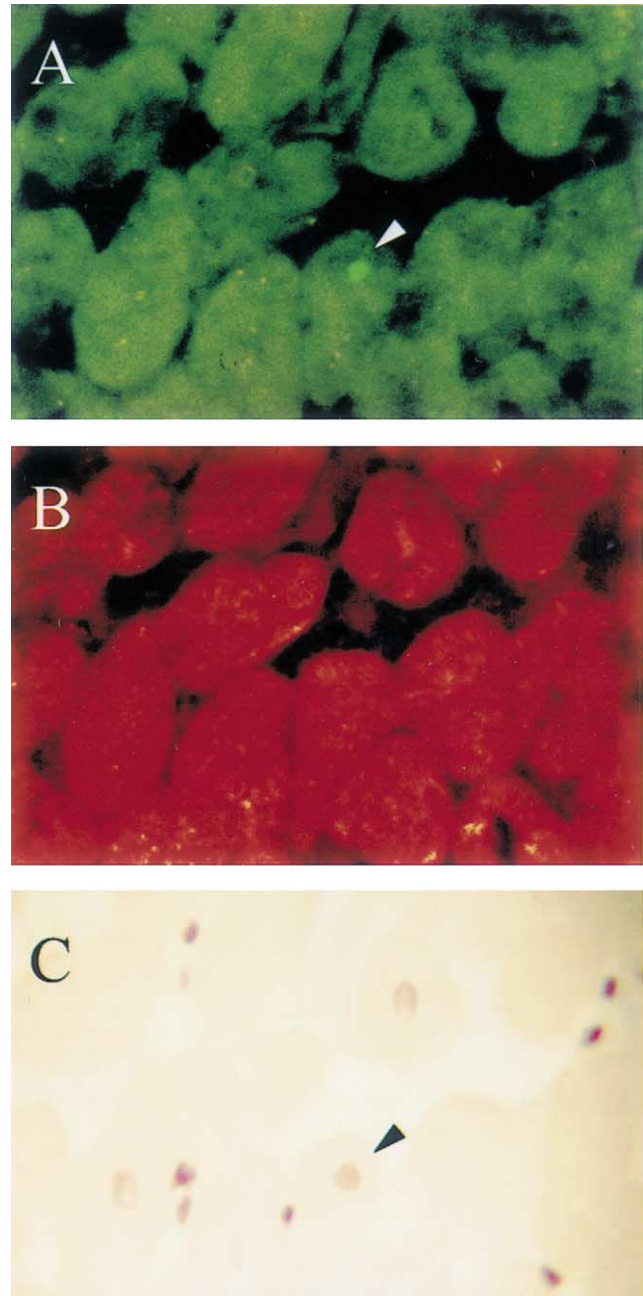


Fig. 2. TUNEL and myosin heavy chain double staining (original magnification $\times 500$). (A) shows a cardiomyocyte nucleus positive labeled by TUNEL (arrow). (B) shows the same LV section as in A stained with anti-myosin heavy chain antibody. B identifies the nucleus referred to in A as that of a cardiomyocyte. Myosin heavy chains are represented as bright spots in the cytoplasm with a red background. (C) Nucleic staining with hematoxylin. The same nucleus in A is stained by hematoxylin (arrow).

cytes, X was the rate of apoptosis, i was the number of 12 h after pacing. Using this calculation, time-dependent increase in total apoptotic cell death was observed after 1, 3 and 4 weeks of pacing (Fig. 3B). By the end of 4 weeks, total number of apoptotic cell death was 1.3×10^8 , which represented 5.4% of LV cardiomyocytes. As

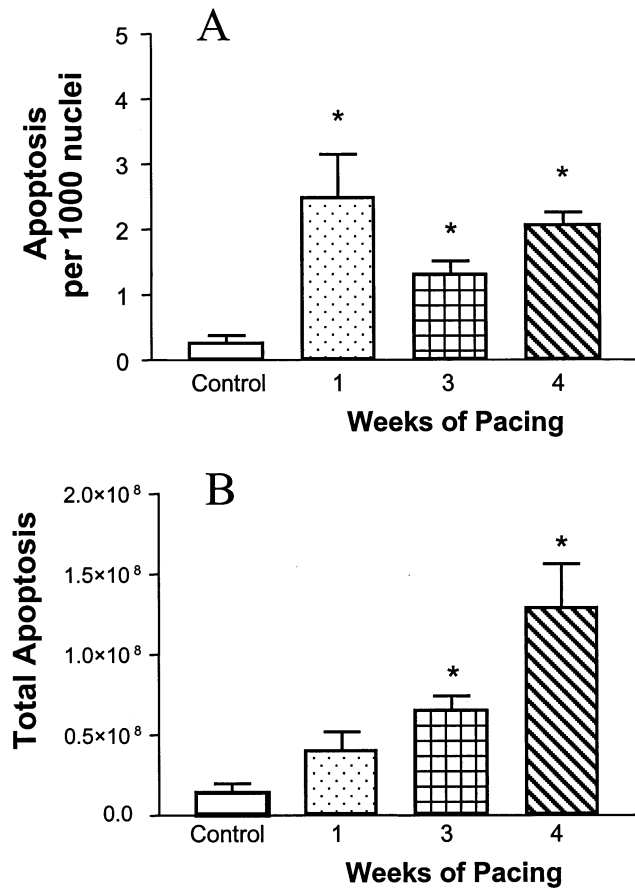


Fig. 3. Myocardial apoptosis in the LV myocardium of pacing-induced heart failure dogs: (A) Percent apoptosis determined by TUNEL at specific time points; (B) Estimated total number of apoptosis over time. $n = 9$ to 14 per group, $*P < 0.05$ vs. controls.

shown in Fig. 4, total cardiomyocyte apoptosis correlated inversely with cardiac output ($r = -0.69$, $P < 0.001$) and directly with LV end diastolic pressure ($r = 0.59$, $P < 0.001$). Plasma norepinephrine correlated significantly with total cardiomyocyte apoptosis ($r = 0.62$, $P < 0.001$, Fig. 5A).

3.5. Protein expression of *bcl-2* and *bax*

Expression of *bcl-2* protein, an inhibitor of apoptosis, was assessed by immunohistochemical staining. *Bcl-2* was not detectable or showed very weak staining in the control dogs. In all groups of paced dogs, there was only weak staining, indicating very limited protein expression. Semi-quantitative grading showed no significant difference among the four groups (differences not significant, Table 2). Western blot analysis showed very weak signals for *bcl-2* protein in all groups. There were no detectable changes after pacing (Fig. 7, upper panel).

Expression of *bax* protein, an inducer of apoptosis, is shown in Fig. 6. Weak *bax* signal was detected in the control dogs. Strong *bax* signal was, however, present in

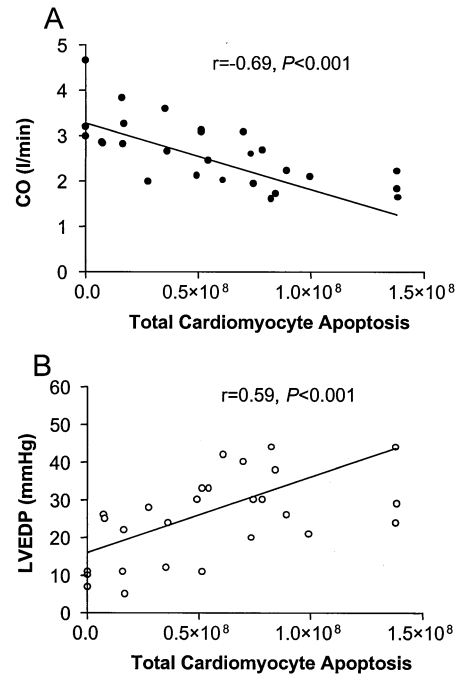


Fig. 4. Relations between the estimated total number of cardiomyocyte apoptosis and myocardial dysfunction. (A) cardiac output (CO) and (B) left ventricular end diastolic pressure (LVEDP).

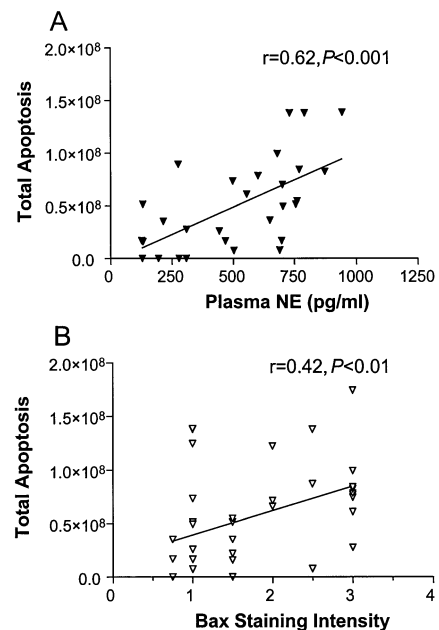


Fig. 5. Correlation between plasma norepinephrine (NE) levels, myocardial *Bax* immunohistochemical staining intensity (semi-quantitative grading) and estimated total cardiomyocyte apoptosis in the ventricles.

all groups of paced dogs. Semi-quantitative grading showed a significant increase in *bax* staining in dogs after 4 weeks of pacing as compared with controls ($P < 0.05$, Table 2). *Bax* staining intensity (grading) correlated with estimated total cardiomyocyte apoptosis ($r =$

Table 2

Semi-quantitative grading of myocardial *bcl-2* and *bax* immunohistochemical staining

| Proteins | Control | 1 week-pacing | 3 week-pacing | 4 week-pacing |
|--------------|-----------|---------------|---------------|------------------------|
| <i>Bcl-2</i> | 0.20±0.13 | 0.33±0.17 | 0.40±0.16 | 0.44±0.18 |
| <i>Bax</i> | 1.13±0.13 | 1.83±0.30 | 1.90±0.27 | 2.25±0.29 ^a |
| <i>n</i> | 10 | 9 | 10 | 10 |

Data are means±S.E.M.

^a $P < 0.05$ vs. controls.

0.42, $P < 0.01$, Fig. 5B). Western blot analysis showed a significant increase in *bax* protein expression in dogs after 3 and 4 weeks of pacing ($P < 0.05$, Fig. 7, lower panel).

3.6. Caspase activities

Caspase activity was measured in all of the control and paced-dogs assessed for TUNEL, *bcl-2* and *bax* as described above. Data for caspase activities of the control and the three groups of paced dogs are shown in Table 3. The detection limit of our assay was 0.15 pmol/μg protein. For purpose of comparing group data, samples from which caspase activities were not detected were assigned a value of 0.15. Caspase activity was not detected in any of the control dogs whereas it was detected in three of the nine dogs paced for 1 week (early heart failure), nine and seven of the 13 and 14 dogs paced for 3 and 4 weeks, respectively, (moderate to severe heart failure). The mean value of caspase activity

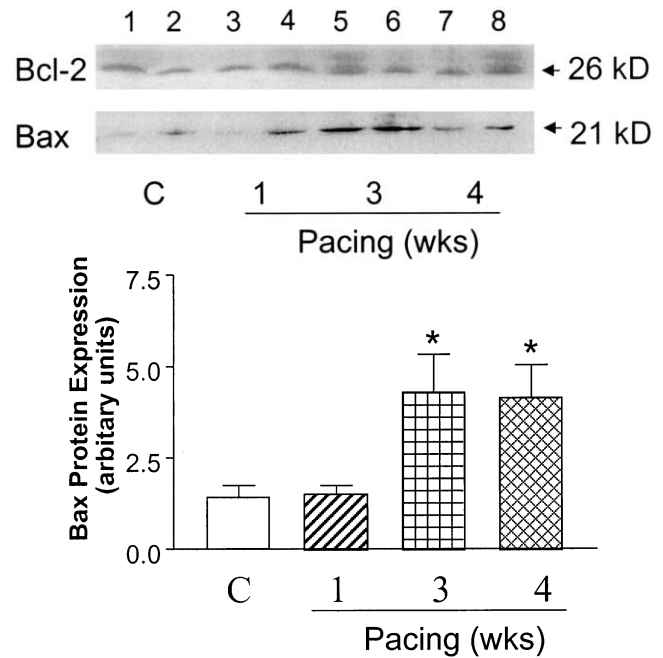


Fig. 7. Western blot analysis of *Bcl-2* and *Bax* protein in the control and dogs paced for 1, 3 and 4 weeks. Upper panel shows representative blots. *Bcl-2* is a 26 kDa protein and *Bax* is a 21 kDa protein. Each lane represents an individual sample. Lower panel shows densitometrical analysis of the *Bax* signals. $n = 6-10$ per group. * $P < 0.05$ vs. controls.

was significantly higher in the dogs paced for 3 and 4 weeks when compared with the controls ($P < 0.05$). Caspase activity did not correlate with estimated total cardiomyocyte apoptosis ($r = 0.24$, not significant).

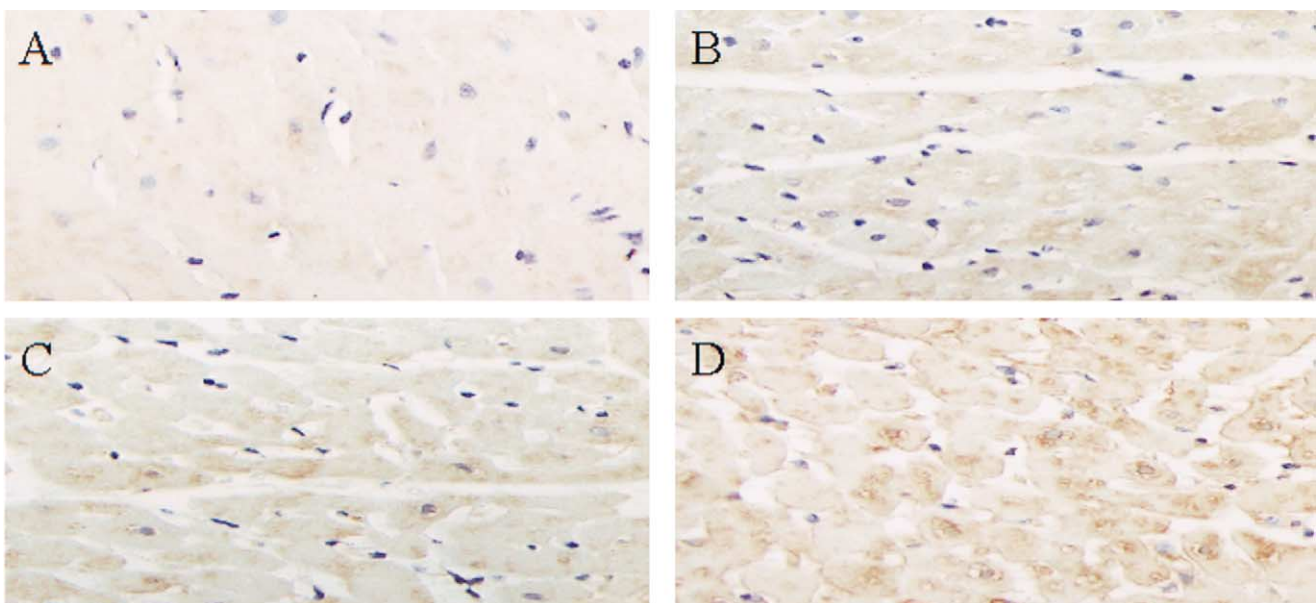


Fig. 6. Immunohistochemical staining of *Bax* protein in the control and dogs paced for 1, 3 and 4 weeks (original magnification $\times 400$). *Bax* staining shows brown in the myocyte cytoplasm. A, controls; B–D, dogs paced for 1, 3 and 4 weeks, respectively.

Table 3
Caspase-3 activity in the myocardium

| pmol/ μ g protein in 2 h | | | | | | | |
|------------------------------|------|-----------------|------|------------------------------|------|------------------------------|------|
| Control | | 1 week-pacing | | 3 week-pacing | | 4 week-pacing | |
| 0.15 | 0.15 | 0.9 | 0.15 | 3.23 | 3.05 | 5.92 | 0.15 |
| 0.15 | 0.15 | 7.18 | | 2.15 | 0.15 | 6.64 | 0.15 |
| 0.15 | | 0.36 | | 3.41 | 0.15 | 3.05 | 4.75 |
| 0.15 | | 0.15 | | 8.08 | 0.15 | 14.54 | 6.02 |
| 0.15 | | 0.15 | | 5.74 | 0.15 | 0.15 | 0.15 |
| 0.15 | | 0.15 | | 0.18 | | 0.15 | 1.83 |
| 0.15 | | 0.15 | | 3.59 | | 0.15 | |
| 0.15 | | 4.75 | | 5.38 | | 0.15 | |
| 0.15 \pm 0 | | 1.04 \pm 0.77 | | 2.72 \pm 0.71 ^a | | 3.32 \pm 1.05 ^a | |

Data are for individual dogs as well as means \pm S.E.M. For comparison of group data, samples not detected with caspase-3 were assigned a value of 0.15, the detection limit of the assay.

^a $P < 0.05$ vs. controls.

4. Discussion

The novel finding of the present study is demonstration in a sequential fashion of persistent myocardial apoptosis from early to advanced heart failure and a significant correlation between myocardial apoptosis and progression of heart failure in a model characterized by progressive increase in hemodynamic stress, neurohormonal and cytokine activation. Furthermore, the expression of *bax* protein, an inducer of apoptosis and the activity of caspases, the executioners of apoptosis, is activated early and persists during evolving heart failure. The results suggest that an early and persistent activation of myocardial apoptosis, *bax* and caspases contribute at least in part to the disease progression in canine pacing-induced cardiomyopathy.

In the dogs with early heart failure (1 week of pacing), there were modest but significant hemodynamic perturbations and increase in plasma norepinephrine level, in the absence of overt clinical signs of heart failure. Although not measured in this study, previous studies had demonstrated that neurohormonal systems such as the renin–angiotensin–aldosterone and endothelin systems were not yet significantly activated at this early stage [13,14,19]. Our dogs with early heart failure, therefore, mimic the neurohormonal profile of patients with asymptomatic LV dysfunction [25]. The lack of a significant increase in LV mass as reported by us and other laboratories [13,17,23] is also an unique and consistent finding for this model and signifies the failure of LV hypertrophy to develop at a whole-organ level. Finally, we observed a progressive increase in plasma TNF- α levels, suggesting a progressive activation of the pro-inflammatory cytokines. The notion is confirmed by our recent data reported by Marin-Garcia (2001) of increased LV tissue TNF- α levels in this model of heart failure [26].

The *bcl-2* family of proteins encompasses a variety of proteins with structural similarities that can initiate or prevent apoptosis [27]. As summarized by Kromer [28], genes identified within this family that can promote cell death are *bax*, *bad*, and *bik*, whereas those that antagonize cell death include *bcl-2*, *bclx_L* and *bcl-W*. In our study, robust protein expression of *bax* as detected by immunohistochemical staining and Western blot analysis was observed in the paced dogs. Although *bcl-2*, the inhibitor of apoptosis was also detected in the paced dogs but not in the control dogs, the differences between the paced and normal dogs in *bcl-2* staining were minimal. Accordingly, in our paced dogs the ratio of *bax* to *bcl-2* was increased during evolving heart failure, rendering the myocytes more predisposed to apoptosis [29]. The significant correlation between *bax* staining and estimated total cardiomyocyte apoptosis observed in the present study further supports this notion. The mechanism for the increase in *bax* to *bcl-2* ratio is unclear. It is possible that hemodynamic stress after pacing may produce sufficient stretch of the myocytes to activate pro-apoptotic factors [30]. Increased *bax* to *bcl-2* ratio alone may not be sufficient to induce apoptosis. Other potentially important factors such as the tumor suppressor gene p53, a transcriptional regulator of *bax* and *bcl-2* gene, as well as other members of the *bcl-2* family may also be involved in the apoptosis process in heart failure [31,32].

Apoptosis as determined by DNA laddering and TUNEL staining was detected in dogs with early heart failure after 1 week of pacing, and in dogs with more severe heart failure. Although the stimulus for apoptosis is most likely to be multi-factorial, it is helpful to relate the onset and degree of apoptosis with those of neurohormone and cytokine activation and hemodynamic stress in our dogs. Communal (1998) has shown that norepinephrine induces apoptosis in the rat ventricular myocytes in vitro [33]. In the present study, plasma norepinephrine levels correlated with the estimated myocardial apoptosis, suggesting that sympathetic activation contributed significantly to the persistence of myocardial apoptosis and, therefore, ongoing myocyte loss. A similar relationship may apply to the pro-inflammatory cytokine TNF- α , an important trigger for apoptosis [34]. Indeed, we have recently demonstrated that TNF- α induces apoptosis in cardiomyocytes [35]. In our dogs, plasma TNF- α level, like plasma norepinephrine level, was increased modestly but significantly in early heart failure and there was further increase in plasma TNF- α level in more severe stages of heart failure. The progressive increase in LV end-diastolic pressures also argued for a relationship between mechanical stress and apoptosis.

The proportion of dUTP-labeled nuclei in our paced dogs (2.5 per thousand nuclei in the 1 week-paced dogs) was comparable to that reported in an earlier study by

Liu on the same canine model [22]. In their study, dogs were paced for 4 weeks and proportion of TUNEL-positive nuclei ranged from 2.9 to 4.5 per thousand myocyte nuclei while only 76 myocytes would be generated in 1 month [22]. Previous studies have demonstrated that cardiomyocyte apoptosis is maximal within 5 h after myocardial ischemia [21] or 12 h after isoproterenol infusion in vivo [23] and 24 h after norepinephrine treatment in vitro [33]. We chose 12 h in our calculation, which in fact represented a conservative estimation. Based on our calculation, apoptosis affected 4.1×10^7 (or a total of 1.7% of myocytes) and 1.3×10^8 (or a total of 5.4%) cardiac myocytes in dogs paced for 1 and 4 weeks, respectively, a number that far exceeded that of myocyte proliferation reported in this model [22]. The fact the apoptotic myocytes far outnumbered proliferating myocytes and the correlation between the total number of apoptotic cell death and the degree of myocardial dysfunction suggest that apoptosis may have contributed at least in part to the progression of heart failure.

Cells undergoing apoptosis following the triggering of 'death receptors' and TNF- α execute the 'death program' by activating a hierarchy of caspases [36]. There are at least 10 caspases in this hierarchy. Caspase-3, -6 and -7 are the executioners of apoptosis. Activation of caspase-3, -6, and -7 is considered a point of no return in the process leading to DNA cleavage and cell destruction [37,38]. In our study, DEVDase activity which represent mainly caspase-3 and -7 activity in the myocardium was not detected in the normal dogs, but was detected in increasing frequency and intensity as one examined in dogs from early to moderately severe and advanced heart failure. Our study was, therefore, the first to demonstrate increased myocardial caspase activity in this model of heart failure and lend further support to the importance of apoptotic cell death in the progression of heart failure. In the present study, myocardial caspase activity did not correlate with estimated total cardiomyocyte apoptosis. The reason for this is not known. It is possible that myocardial apoptosis is executed by caspase-6, or a combination of caspase-3, -6 and -7 or caspase-independent pathway such as oxidative stress may be involved in this model of heart failure. Finally, besides the TNF- α mediated death receptor pathway, TNF- α and increased oxidative stress could both impair mitochondrial function, leading to increased cytochrome *c* and caspases, which in turn triggers apoptosis [39,40]. To support this notion, we have also demonstrated recently in this model impaired mitochondrial function in association with increased LV oxidative stress and TNF- α level [26]. On the other hand, it should be recognized that TNF- α may also inhibit apoptosis via the stimulation of NF- κ B [41]. The relative contribution of each pathway cannot be discerned in this study.

Several aspects of our study warrant further discussion. First, technological limitations are inherent to the TUNEL and other labeling methods [42]. Second, total number of apoptotic cell death in each group was not directly measured but rather estimated based on several assumptions as outlined. Third, it is impossible to ascertain whether 5.4% of myocytes undergoing apoptosis, estimated in our study, is sufficient to cause progression of heart failure. However, one can be reasonably certain that this number far exceeded the myocyte mitotic rate reported in dogs with pacing-induced heart failure or patients with dilated cardiomyopathy [22,43]. Fourth, the correlation between myocardial apoptosis and progressive deterioration of heart function does not necessarily prove a cause-effect relationship between myocardial apoptosis and cardiac dysfunction. Finally, while apoptotic cell death may account in part for the lack of whole-organ LV hypertrophy in this model, other mechanisms such as exhaustion of energy substrate [44] and alterations in the collagen matrix [45] may also play an important role. Future studies using effective anti-apoptosis therapies such as caspase inhibitors may provide evidence for a definitive relationship between myocyte apoptosis and pump dysfunction.

5. Conclusion

The present study demonstrates that apoptotic cells are markedly increased after 1 week of pacing and remain increased at 4 weeks of pacing. Increases in apoptosis are associated with increased *bax* protein expression and caspase activation. The estimated total number of apoptotic cells correlates with the degree of cardiac dysfunction. We conclude that an early and persistent activation of myocardial apoptosis likely contribute to the progression of heart failure in the canine model of pacing-induced cardiomyopathy.

Acknowledgements

This study was supported by grants from the Heart and Stroke Foundation of Ontario (T-4045) and the Canadian Institutes of Health Research (MT-14653), Canada. Dr Qingping Feng was supported by a Research Career Award in Health Sciences from the Pharmaceutical Manufacturer's Association of Canada Health Research Foundation and the Canadian Institutes of Health Research.

References

- [1] J.B. O'Connell, M.R. Bristow, Economic impact of heart failure in the United States: time for a different approach, *J. Heart Lung Transplant* 13 (1994) S107–S112.
- [2] M. Packer, Neurohormonal interactions and adaptations in congestive heart failure, *Circulation* 77 (1988) 721–730.
- [3] G. Torre-Amione, S. Kapadia, J. Lee, J.B. Durand, R.D. Bies, J.B. Young, D.L. Mann, Tumor necrosis factor- α and tumor necrosis factor receptors in patients in the failing human heart, *Circulation* 93 (1996) 704–711.
- [4] M.J. Arend, A.H. Wyllie, Apoptosis: mechanisms and roles in pathology, *Int. Rev. Exp. Pathol.* 32 (1991) 223–254.
- [5] S. Nagata, P. Goldstein, The Fas death factor, *Science* 267 (1995) 1449–1456.
- [6] E. Yonish-Rouach, D. Resnitzky, J. Lotem, L. Sach, A. Kimchi, M. Oren, Wild-type p53 induces apoptosis of myeloid leukemic cells that is inhibited by interleukin-6, *Nature* 352 (1991) 345–347.
- [7] M. Hanada, C. Aime-Sempe, T. Sato, J.C. Reed, Structure-function analysis of *bcl-2* protein: identification of conserved domains important for homodimerization with *bcl-2* and heterodimerization with *bax*, *J. Biol. Chem.* 270 (1995) 11962–11969.
- [8] N. Itoh, J. Tamura, S. Dagata, Effect of *bcl-2* on Fas antigen-mediated cell death, *J. Immunol.* 151 (1993) 621–627.
- [9] H. Fliss, D. Gatteringer, Apoptosis in ischemic and reperfused rat myocardium, *Circ. Res.* 76 (1996) 949–956.
- [10] S. Bialik, D.L. Geenen, I.E. Sasson, R. Cheng, J.W. Horner, S.M. Evans, E.M. Lord, C.J. Koch, R.N. Kitsis, Myocyte apoptosis during acute myocardial infarction in the mouse localizes to hypoxic regions but occurs independently of p53, *J. Clin. Invest.* 100 (1997) 1363–1372.
- [11] J. Narula, N. Haider, R. Virmani, T.G. DiSalvo, F.D. Kolodgie, R.J. Hajjar, U. Schmidt, M.J. Semigran, G.W. Dec, B.A. Khaw, Apoptosis in myocytes in end stage heart failure, *New Engl. J. Med.* 335 (1996) 1182–1189.
- [12] G. Olivetti, R. Abbi, F. Quaini, J. Kajstura, W. Cheng, J.A. Nitahara, E. Quaini, C. Di Loreto, C.A. Beltrami, S. Krajewski, J.C. Reed, P. Anversa, Apoptosis in the failing human heart, *New Engl. J. Med.* 336 (1997) 1131–1141.
- [13] P.W. Armstrong, G.W. Moe, The development and recovery from pacing-induced heart failure, in: F.G. Spinale (Ed.), *Pathophysiology of Tachycardia-Induced Heart Failure*, Futura Publishing Company, Armonk, NY, 1996, pp. 45–49.
- [14] G.W. Moe, P.W. Armstrong, Pacing-induced heart failure: a model to study the mechanism of disease progression and novel therapy in heart failure, *Cardiovasc. Res.* 42 (1999) 591–599.
- [15] K.A. Krown, M.T. Page, C. Ngugen, D. Zechner, V. Gutierrez, K.L. Comstock, C.C. Glembotski, P.J. Quintana, R.A. Sabbadini, Tumor necrosis factor α -induced apoptosis in cardiac myocytes. Involvement of the sphingolipid signaling cascade in cardiac cell death, *J. Clin. Invest.* 98 (1996) 2854–2865.
- [16] P.W. Armstrong, T.P. Stopps, S.E. Ford, A.J. de Bold, Rapid ventricular pacing in the dog: pathophysiologic studies of heart failure, *Circulation* 74 (1986) 1075–1084.
- [17] R.J. Howard, G.W. Moe, P.W. Armstrong, Sequential echocardiographic-doppler assessment of left ventricular remodeling and mitral regurgitation during evolving experimental heart failure, *Cardiovasc. Res.* 25 (1991) 468–474.
- [18] H.L. Wyatt, M.K. Heng, S. Meerbaum, J.D. Hestenes, J.M. Cobo, R.M. Davidson, E. Corday, Cross sectional echocardiography, Part 1. Analysis of mathematical model for quantifying mass of the left ventricle in dogs, *Circulation* 60 (1979) 1104–1113.
- [19] G.W. Moe, E.A. Grima, C. Angus, N.L. Wong, D.C. Hu, R.J. Howard, P.W. Armstrong, Response of atrial natriuretic factor to acute and chronic increases of atrial pressures in experimental heart failure in dogs, *Circulation* 83 (1991) 1780–1787.
- [20] J.L. Tilly, A.J.W. Hsueh, Microscale autoradiographic method for the qualitative and quantitative analysis of apoptotic DNA fragmentation, *J. Cell. Physiol.* 154 (1993) 519–526.
- [21] J. Kajstura, W. Cheng, K. Reiss, E. Szoke, W. Cheng, G. Olivetti, T.H. Hintze, P. Anversa, Apoptotic and necrotic cell deaths are independent contributing variables of infarct size in rats, *Lab. Invest.* 74 (1996) 86–107.
- [22] Y. Liu, E. Cigola, W. Cheng, J. Kajstura, G. Olivetti, T.H. Hintze, P. Anversa, Myocyte nuclear mitotic division and programmed myocyte cell death characterize the cardiac myopathy induced by rapid ventricular pacing in dogs, *Lab. Invest.* 73 (1995) 771–787.
- [23] J. Kajstura, X. Zhang, Y. Liu, E. Szoke, W. Cheng, G. Olivetti, T.H. Hintze, P. Anversa, The cellular basis of pacing-induced dilated cardiomyopathy. Myocyte cell loss and myocyte cellular reactive hypertrophy, *Circulation* 92 (1995) 2306–2317.
- [24] Y. Shizukuda, P.M. Buttrick, D.L. Geenen, A.C. Borczuk, R.N. Kitsis, E.H. Sonnenblick, Adrenergic stimulation causes cardiocyte apoptosis: influence of tachycardia and hypertrophy, *Am. J. Physiol.* 275 (1998) H961–H968.
- [25] C.R. Benedict, B. Shelton, D.E. Johnstone, G. Francis, B. Greenberg, M. Konstam, J.L. Probstfield, S. Yusuf, Prognostic significance of plasma norepinephrine in patients with asymptomatic left ventricular dysfunction, *Circulation* 94 (1996) 690–697.
- [26] J. Marin-Garcia, M.J. Goldenthal, G.W. Moe, Cardiac and skeletal muscle mitochondrial dysfunction in pacing-induced cardiac failure, *Cardiovasc. Res.* 52 (2001) 103–110.
- [27] H.-G. Wang, U.R. Rapp, J.C. Reed, *Bcl-2* targets the protein kinase *Raf-2* to mitochondria, *Cell* 87 (1996) 629–638.
- [28] G. Kromer, The proto-oncogene *bcl-2* and its role in regulating apoptosis, *Nat. Med.* 3 (1997) 614–620.
- [29] T. Miyashita, S. Krajewski, M. Krajewski, H.G. Wang, H.K. Lin, D.A. Liebermann, B. Hoffman, J.C. Reed, Tumor suppressor p53 is a regulator of *bcl-2* and *bax* gene expression in vitro and in vivo, *Oncogene* 9 (1994) 1799–1805.
- [30] W. Cheng, B. Li, J. Kajstura, M.S. Wolin, E.H. Sonnenblick, T.H. Hintze, G. Olivetti, P. Anversa, Stretch-induced programmed myocyte cell death, *J. Clin. Invest.* 96 (1995) 2247–2259.
- [31] T. Miyashita, J.C. Reed, Tumor suppressor p53 is a direct transcriptional activator of the human *bax* gene, *Cell* 80 (1995) 293–299.
- [32] A. Leri, A. Malhorta, Q. Li, Q. Li, P. Stiegler, P.P. Claudio, A. Giordano, J. Kajstura, T.H. Hintze, P. Anversa, Pacing-induced heart failure dogs enhances the expression of p53 and p53-dependent genes in ventricular myocytes, *Circulation* 97 (1998) 194–203.
- [33] C. Communal, K. Singh, D.R. Pinmentel, W.S. Colucci, Norepinephrine stimulates apoptosis in the adult rat ventricular myocytes by activation of the β -adrenergic pathway, *Circulation* 98 (1998) 1329–1334.
- [34] K.A. Krown, M.T. Page, C. Ngugen, D. Zechner, V. Gutierrez, K.L. Comstock, C.C. Glembotski, P.J. Quintana, R.A. Sabbadini, Tumor necrosis factor α -induced apoptosis in cardiac myocytes. Involvement of the sphingolipid signaling cascade in cardiac cell death, *J. Clin. Invest.* 98 (1996) 2854–2865.
- [35] W. Song, X. Lu, Q. Feng, Tumor necrosis factor- α induces apoptosis in cardiac myocytes via inducible nitric oxide synthase in neonatal mouse cardiomyocytes, *Cardiovasc. Res.* 45 (2000) 595–602.
- [36] G.M. Cohen, Caspases: the executioner of apoptosis, *Biochem. J.* 326 (1997) 1–16.
- [37] M. Enari, H. Sakahira, H. Yokoyama, K. Okawa, A. Iwamatsu, S. Nagata, A caspase-activated DNase that degrades DNA during apoptosis, and its inhibitor ICAD, *Nature* 391 (1998) 43–50.

- [38] S.M. Schwartz, Cell death and the caspase cascade, *Circulation* 97 (1998) 227–229.
- [39] J. Marin-Garcia, M.J. Goldenthal, G.W. Moe, Mitochondrial pathology in cardiac failure, *Cardiovasc.Res.* 49 (2001) 17–26.
- [40] J.C. Reed, Cytochrome *c*: can't live with it—can't live without it, *Cell* 91 (1997) 559–562.
- [41] A.A. Beg, D. Baltimore, An essential role for NF-kappaB in preventing TNF-alpha-induced cell death, *Science* 274 (1996) 782–784.
- [42] J. Schaper, A. Elasser, S. Kostin, The role of cell death in heart failure, *Circ. Res.* 85 (1999) 867–869.
- [43] J. Kajstura, A. Leri, N. Finato, C. Di Loreto, C.A. Beltrami, P. Anversa, Myocyte proliferation in end-stage cardiac failure in humans, *Proc. Natl. Acad. Sci. USA* 95 (1998) 8801–8805.
- [44] P.J. O'Brien, C.D. Ianuzzo, G.W. Moe, T.P. Stopps, P.W. Armstrong, Rapid ventricular pacing of dogs to heart failure: biochemical and physiological studies, *Can. J. Physiol. Pharmacol.* 68 (1990) 34–39.
- [45] P.W. Armstrong, G.W. Moe, R.J. Howard, E.A. Grima, T.F. Cruz, Structural remodelling in heart failure: gelatinase induction, *Can. J. Cardiol.* 10 (1994) 214–220.